

# Higher-Order Poincaré Sphere, Stokes Parameters, and the Angular Momentum of Light

Giovanni Milione,<sup>1</sup> H. I. Sztul,<sup>1</sup> D. A. Nolan,<sup>2</sup> and R. R. Alfano<sup>1,\*</sup>

<sup>1</sup>The City College of New York of the City University of New York, 160 Convent Avenue New York, New York 10031, USA

<sup>2</sup>Corning Incorporated, Sullivan Park, Corning, New York 14831, USA

(Received 21 March 2011; published 25 July 2011)

A higher-order Poincaré sphere and Stokes parameter representation of the higher-order states of polarization of vector vortex beams that includes radial and azimuthal polarized cylindrical vector beams is presented. The higher-order Poincaré sphere is constructed by naturally extending the Jones vector basis of plane wave polarization in terms of optical spin angular momentum to the total optical angular momentum that includes higher dimensional orbital angular momentum. The salient properties of this representation are illustrated by its ability to describe the higher-order modes of optical fiber waveguides, more exotic vector beams, and a higher-order Pancharatnam-Berry geometric phase.

DOI: 10.1103/PhysRevLett.107.053601

PACS numbers: 42.50.Tx, 03.65.Vf, 42.25.Ja, 42.81.-i

Polarization is one of light's most salient features, even more so than its spectral or coherence properties [1]. A prominent geometric representation of polarization came in 1892 when Poincaré showed that the state of polarization (SOP) of a light beam can be described as a point on the surface of a unit sphere now known as the Poincaré sphere (PS) (Fig. 1) [2]. The PS unifies all of the fundamental polarization descriptors, where the SOP as represented by a complex Jones vector is mapped to the sphere's surface through the Stokes parameters (SPs) as the sphere's Cartesian coordinates [1]. This geometric connection provides not only remarkable insight into but also greatly simplifies otherwise complex polarization problems, and as a result has become an ubiquitous device with which to treat polarization phenomena in numerous and varying fields.

Despite this powerful utility, the SOPs represented by the PS in its current form are limited to the simplest and most fundamental homogenous plane wave solutions of Maxwell's vector wave equation. Most recently there has been increasing interest in higher-order solutions which admit spatially inhomogeneous SOPs such as in the cylindrically symmetric coordinate systems of laser cavity resonators and fiber optic waveguides [3]. Of particular interest are the vectorial vortex (VV) beams also referred to as spirally polarized beams [4] such as radial and azimuthal polarized cylindrical vector (CV) beams [5] and their optical fiber analogs the  $TM_{01}$  and  $TE_{01}$  fiber modes [6], respectively. They extend the properties of more conventional plane wave SOPs such as in their ability to produce strong longitudinal field components and smaller waist sizes upon focusing by high numerical aperture objectives [7]. This has been exploited in applications such as spectroscopy [8], particle acceleration [9], microscopy [10], and optical trapping [11], to name a few. These higher-order SOPs also naturally arise in crystal optics [12], Mie scattering [13], cosmic background radiation [14], and are related to the  $C$ -point organizing symmetries in the field

of singular optics [15]. As such, a representation of the VV beams in the framework of the PS would offer great utility. In this Letter, it is shown that the PS can be extended to a higher-order PS representation of the higher-order SOPs of VV beams. Higher-order SPs are also derived and discussed. The salient properties of this higher-order representation are discussed and its utility demonstrated in its ability to describe the higher-order modes of optical fiber waveguides, other exotic vector beams, and a higher-order Pancharatnam-Berry geometric phase (GP).

The PS elucidates the rich connection between optical angular momentum (AM) and a light beam's SOP. As suggested by Poynting [16] and demonstrated by Beth [17], light can possess a spin angular momentum (SAM)

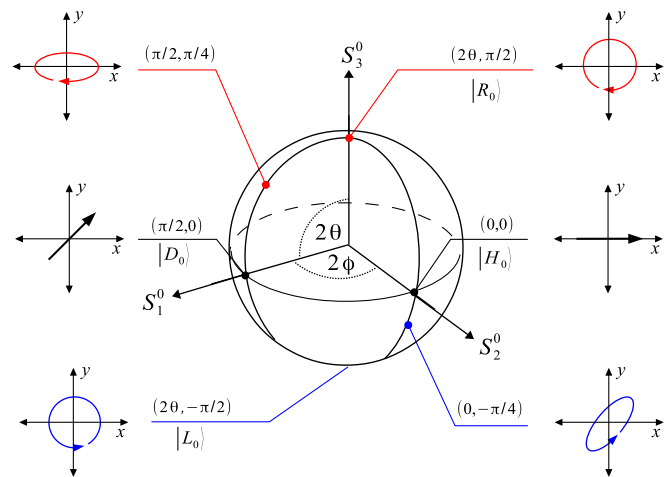


FIG. 1 (color online). Poincaré sphere representation for plane wave states of polarization. The poles represent right and left circular polarization, the equator linear polarization, and intermediate points between the poles and equator elliptical polarization. The northern and southern hemispheres separate right (red) and left (blue) handed ellipticity. Antipodal points are orthogonal, and any state of polarization is given as their linear combination.

of  $\sigma\hbar$  ( $\sigma = \pm 1$ ) per photon associated with circular polarization (CP). The poles of the PS then represent the optical SAM eigenstates, which in turn form the constituent components of any plane wave SOP. Light can carry in addition to its SAM a higher dimensional orbital angular momentum (OAM) of  $\ell\hbar$  ( $\ell = \pm 1, \pm 2, \pm 3, \dots$ ) per photon associated with a helical wave front described by the azimuthal phase factor  $\exp(\pm i\ell\varphi)$  called an optical vortex (OV),  $\varphi = \arctan(y/x)$  being the azimuthal coordinate [18]. The integer  $\ell$  is referred to as the topological charge and describes the number of the vortices'  $2\pi$  helical phase windings in one wavelength. For paraxial light beams, the SAM and OAM are additive, with a total optical AM per photon of  $J = (\ell + \sigma)\hbar$ . The SOPs of VV beams are a linear combination of orthogonal CP OVs of opposite topological charge [19] where the constituent components are eigenstates of the total optical AM. For a monochromatic paraxial light beam this can be represented as a two-dimensional Jones vector given by the equation

$$|\psi_\ell\rangle = \psi_R^\ell |R_\ell\rangle + \psi_L^\ell |L_\ell\rangle, \quad (1)$$

with respect to the orthonormal *circular* polarization basis  $\{|R_\ell, L_\ell\rangle$  [20] such that

$$|R_\ell\rangle = \exp(-i\ell\varphi)(\hat{\mathbf{x}} + i\hat{\mathbf{y}})/\sqrt{2}, \quad (2)$$

$$|L_\ell\rangle = \exp(+i\ell\varphi)(\hat{\mathbf{x}} - i\hat{\mathbf{y}})/\sqrt{2}. \quad (3)$$

Equations (1) and (2) represent a right circular polarized (RCP) and left circular polarized (LCP) OV of topological charge  $-\ell$  and  $+\ell$ , respectively. Equation (1) can also be expressed with respect to the horizontal and vertical polarization basis  $\{|H_\ell, V_\ell\rangle$  through the relations  $|H_\ell\rangle = (|R_\ell\rangle + |L_\ell\rangle)/2$  and  $|V_\ell\rangle = -i(|R_\ell\rangle - |L_\ell\rangle)/2$ , where

$$|V_\ell\rangle = \cos(\ell\varphi)\hat{\mathbf{x}} + \sin(\ell\varphi)\hat{\mathbf{y}}, \quad (4)$$

$$|H_\ell\rangle = -\sin(\ell\varphi)\hat{\mathbf{x}} + \cos(\ell\varphi)\hat{\mathbf{y}}, \quad (5)$$

with coefficients  $\psi_H^\ell = (\psi_R^\ell + \psi_L^\ell)$  and  $\psi_V^\ell = i(\psi_R^\ell - \psi_L^\ell)$ , as well as the diagonal and antidiagonal polarization basis  $\{|D_\ell, A_\ell\rangle$  through the relations  $|D_\ell\rangle = (|H_\ell\rangle + |V_\ell\rangle)/\sqrt{2}$  and  $|A_\ell\rangle = (|H_\ell\rangle - |V_\ell\rangle)/\sqrt{2}$ , where

$$|D_\ell\rangle = \cos(\ell\varphi + \pi/4)\hat{\mathbf{x}} + \sin(\ell\varphi + \pi/4)\hat{\mathbf{y}}, \quad (6)$$

$$|A_\ell\rangle = \sin(\ell\varphi + \pi/4)\hat{\mathbf{x}} - \cos(\ell\varphi + \pi/4)\hat{\mathbf{y}}, \quad (7)$$

with coefficients  $\psi_D^\ell = (\psi_H^\ell + \psi_V^\ell)/\sqrt{2}$  and  $\psi_A^\ell = (\psi_H^\ell - \psi_V^\ell)/\sqrt{2}$ . For  $\ell = 0$ , the bases of Eqs. (2)–(7) reduce to the standard plane wave SOP bases. For  $\ell \geq 1$ , the VV beam of Eq. (1) is characterized by the existence of an on-axis polarization singularity of topological charge  $\ell$  referred to as a *V* point [21]. Beams of this nature include vector Laguerre-Gaussian (LG<sub>p</sub><sup>ℓ</sup>) laser modes, even those of higher radial order ( $p \geq 1$ ) [19,22].

Normalized higher-order SP in the *circular* basis of Eqs. (2) and (3) are given by [23]

$$S_0^\ell = |\langle R_\ell | \psi \rangle|^2 + |\langle L_\ell | \psi \rangle|^2 = |\psi_R^\ell|^2 + |\psi_L^\ell|^2, \quad (8)$$

$$S_1^\ell = 2 \operatorname{Re}(\langle R_\ell | \psi \rangle^* \langle L_\ell | \psi \rangle) = 2|\psi_R^\ell||\psi_L^\ell| \cos\phi, \quad (9)$$

$$S_2^\ell = 2 \operatorname{Im}(\langle R_\ell | \psi \rangle^* \langle L_\ell | \psi \rangle) = 2|\psi_R^\ell||\psi_L^\ell| \sin\phi, \quad (10)$$

$$S_3^\ell = |\langle R_\ell | \psi \rangle|^2 - |\langle L_\ell | \psi \rangle|^2 = |\psi_R^\ell|^2 - |\psi_L^\ell|^2, \quad (11)$$

where  $\phi = \arg(\psi_R^\ell) - \arg(\psi_L^\ell)$  and  $(S_0^\ell)^2 \leq (S_1^\ell)^2 + (S_2^\ell)^2 + (S_3^\ell)^2$ . A fully polarized beam is considered such that  $S_0^\ell = 1$ , yet this formalism may describe unpolarized or partially polarized VV beams where  $S_0^\ell < 1$ . For  $\ell = 0$ , the SP components of Eqs. (8)–(11) reduce to the standard plane wave SP components.  $S_0^\ell$  represents the total beam intensity where  $|\psi_R^\ell|^2$  and  $|\psi_L^\ell|^2$  are the intensities of Eqs. (2) and (3), respectively, and  $S_3^\ell$  the beam content of each. This equivalently represents the overall degree of ellipticity of the VV beam analogous to the degree of ellipticity of a plane wave SOP described by the standard SPs.  $S_1^\ell$  and  $S_2^\ell$  contain the relative phase information  $\phi$  between the RCP OV and LCP OV of Eqs. (2) and (3), respectively. This equivalently represents the relative polarization orientation of the VV beam analogous to the orientation of a plane wave SOP described by the standard SPs.

Experimental measurement of the higher-order SPs can be carried out analogous to the technique of Stokes polarimetry for the standard SPs, which is effectively a measurement of the optical SAM content of a beam using a linear polarizer and quarter wave plate [1]. For the higher-order SOPs of VV beams, the optical OAM associated with the topological charge of the OVs must also be measured. This can be accomplished using conventional optical elements such as a  $\pi/2$  cylindrical lens mode converter and fork diffraction grating to perform the equivalent operation of the linear polarizer and quarter wave plate, respectively [24]. The VV beams form a direct product space between the optical SAM and OAM subspaces and therefore their experimental measurement through the higher-order SPs requires their decomposition into these parts. A detailed analysis of this experimental measurement is the subject of a future paper. It should be noted that the *V*-point polarization singularity of the VV beams results in an on-axis intensity null. Equations (8)–(11) take this into account through the measurement of the topological charge of the OVs proposed above. The higher-order SPs then may offer an additional way to describe polarization singularities beyond the standard SPs [15].

The higher-order PS is constructed using  $S_1^\ell$ ,  $S_2^\ell$ , and  $S_3^\ell$  as the sphere's Cartesian coordinates with  $S_0^\ell$  the unit radius from the origin and the sphere's spherical angles  $(2\theta, 2\phi)$  given by [1]

$$2\theta = \tan^{-1}(S_2^\ell/S_1^\ell), \quad (12)$$

$$2\phi = \sin^{-1}(S_3^\ell/S_0^\ell). \quad (13)$$

The resulting sphere describes a higher-order VV SOP at each point  $(2\theta, 2\phi)$  along the surface where the sphere's poles represent CP OVs—the total optical AM eigenstates, the equator represents VV SOPs that are linear polarized everywhere, and intermediate points between the poles and equator represent elliptically polarized VV SOPs. This higher-order PS has two salient features: (1) For  $\ell = 0$  the higher-order PS reduces to the standard plane wave PS, which is only a *zeroth* order representation. (2) For  $\ell \geq 1$  the OV and CP handedness of each pole can be in the same,  $|\ell| = |\sigma|$ , or opposite,  $|\ell| \neq |\sigma|$ , sense and therefore in the higher-order basis *two spheres* must be described.

This is illustrated in Figs. 2 and 3 for  $\ell = \pm 1$  higher-order PSs. For  $\ell = +1$  shown in Fig. 2, the higher-order PS can completely characterize a general CV beam SOP [5] such as radial and azimuthal polarization which is equivalent to the  $TE_{01}$  and  $TM_{01}$  fiber modes. For  $\ell = -1$  shown in Fig. 3, the higher-order PS can describe the so-called  $\pi$ -vector beams [11] which is equivalent to the  $HE_{21}^{\text{odd}}$  and  $HE_{21}^{\text{even}}$  fiber modes. This representation holds for spheres of  $\ell > |\pm 1|$ .

The utility of the higher-order PS is illustrated by its ability to describe the higher-order polarization phenomenon of an optical fiber waveguide. Considering a weakly

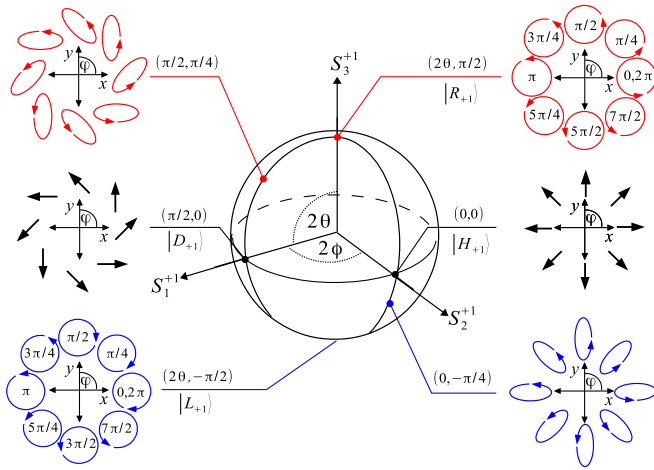


FIG. 2 (color online). Higher-order PS representation for  $(|\ell| \neq |\sigma|; \ell = +1)$ : The poles  $(2\theta, \pm\pi/2)$  represent orthogonal CP  $\ell = \pm 1$  OVs. Equatorial points  $(\theta, 0)$  represent generalized CV beams [5] including the horizontal and vertical basis of Eqs. (4) and (5),  $(0, 0)$  and  $(\pi, 0)$  that represents radial and azimuthal or equivalently the  $TM_{01}$  and  $TE_{01}$  fiber modes, respectively, and the diagonal and antidiagonal basis of Eqs. (6) and (7),  $(\pi/2, 0)$  and  $(3\pi/4, 0)$ , that represents spiral polarization [4]. Intermediate points between the poles and equator represent elliptically polarized CV beams.

guiding, step index, circular core fiber that supports up to the  $LP_{01}$  mode [6], excitation of all the modes within the fiber can be expressed in terms of Eqs. (4) and (5) as

$$\sum_{\ell} |\psi_{\ell}\rangle = \sum_{\ell=-1}^{\ell=+1} (\psi_H^{\ell} |H_{\ell}\rangle + \psi_V^{\ell} |V_{\ell}\rangle), \quad (14)$$

where  $|H_0\rangle = HE_{11}^{\text{odd}}$ ,  $|V_0\rangle = HE_{11}^{\text{even}}$ ,  $|V_{+1}\rangle = TE_{01}$ ,  $|H_{+1}\rangle = TM_{01}$ ,  $|V_{-1}\rangle = HE_{21}^{\text{odd}}$ , and  $|H_{-1}\rangle = HE_{21}^{\text{even}}$ . Representation by the higher-order PS of Eq. (14) is accomplished by using a superposition of spheres for  $\ell = 0$ ,  $\ell = +1$ , and  $\ell = -1$ . The state  $|\psi_{\ell}\rangle$  on each sphere represents a linear combination of the respective fiber modes, where  $|\psi_H^{\ell}|$  and  $|\psi_V^{\ell}|$  are interpreted as amplitude of each fiber mode, and  $\arg(\psi_H^{\ell})$  and  $\arg(\psi_V^{\ell})$  their propagation constants. This can be measured at the fiber output through the measurement of the higher-order Stokes parameters. This same approach may be used to represent more exotic vector beams such as the full Poincaré beams [25], hybrid vector beams [26], or double-mode vector beams [19,22]. This representation may fall short of representing any arbitrary vector beam such as those with radial-variant SOP [27]. While these beams are novel in and of themselves, they need not apply to this representation because their constituent components are not eigenstates of the total optical AM.

The higher-order PS can also illustrate a higher-order Pancharatnam-Berry GP  $\phi_g$ . First shown by Pancharatnam [28], a plane wave SOP taking a cyclic path on the standard PS acquires a phase directly proportional to half the area  $\Omega/2$  subtended by the circuit. On the higher-order PS, this is equivalent to a CP OV taking a geodesic from north to

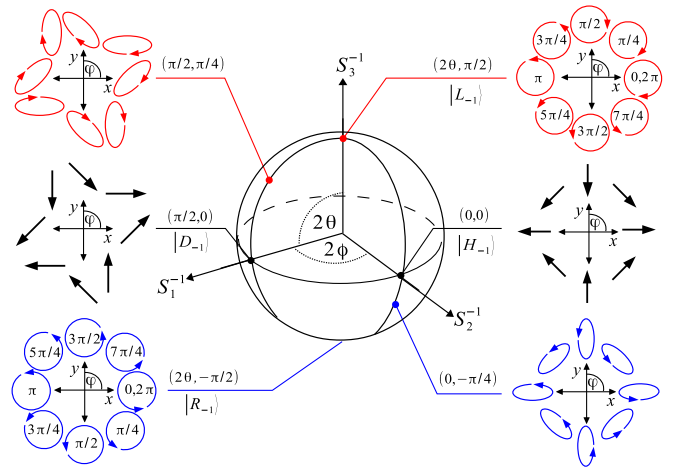


FIG. 3 (color online). Higher-order PS representation for  $(|\ell| = |\sigma|; \ell = -1)$ : The poles  $(2\theta, \pm\pi/2)$  represent orthogonal CP  $\ell = \pm 1$  OVs. Equatorial points  $(\theta, 0)$  represent  $\pi$ -vector beams [11]. The horizontal and vertical basis of Eqs. (4) and (5),  $(0, 0)$  and  $(\pi, 0)$ , represent  $\pi$ -radial and  $\pi$ -azimuthal vector beams, respectively, and equivalently the  $HE_{21}^{\text{odd}}$  and  $HE_{21}^{\text{even}}$  optical fiber modes. Intermediate points between the poles and equator describe elliptically polarized  $\pi$ -vector beams.

south pole and then back, which can be physically carried out using two half wave plate- $\pi$ -cylindrical lens mode converter *pairs* through the angle of rotation  $\phi$  of the second *pair* [29]. This transformation can be analyzed using the Jones matrix formalism for a light beam bearing both SAM and OAM [24] where using the corresponding Jones matrices for the pairs it is easily shown that the initial CP OV acquires an additional phase factor proportional to  $(\ell + \sigma)2\phi$ , which is the GP, the constant of proportionality being only a sign factor. From a basic geometric visualization of this transformation on the sphere, it is seen that the angle of rotation of the second pair  $\phi$  is equivalent to a rotation of  $2\phi$  about the sphere's polar axis which in turn sweeps out between the geodesic paths the solid angle  $2\phi = \Omega/2$ . The resulting GP on the higher-order PS is then given by

$$\phi_g \propto (\ell + \sigma)\Omega/2. \quad (15)$$

This argument obeys the 2-to-1 homeomorphism between the SU(2) space of the Jones calculus and the SO(3) space of the PS which has similarly been made by Bhandari and Samuel [30] and Simon *et al.* [31] in regard to the GP on the standard PS. The GP of Eq. (15) scales is additive between the optical SAM and OAM as expected since the higher-order PS is the direct product space between the optical SAM and OAM subspaces where the half wave plate and  $\pi$ -cylindrical lens mode converter effect each, respectively. For the higher-order PS representation of two spheres, it may be interesting to explore the properties of this GP in, for example, jumps between spheres which can be carried out by a single pair, or in the context of Berry's argument that the GP is due to the flux of an artificial magnetic monopole situated at the PS origin [32,33]. A more detailed analysis and an experimental verification are the subject of a future paper.

In conclusion, a higher-order PS representation of the higher-order SOPs of VV beams has been presented. The higher-order PS has been constructed by naturally extending the basis of polarization in terms of the optical SAM to the total optical AM that includes the higher dimensional OAM. Higher-order SP have been derived and discussed in terms of a light beam's measurable decomposition into optical SAM and OAM parts. The higher-order PS representation reduces to the standard plane wave PS, shown to be a zeroth order representation, and a degeneracy into two spheres. The utility of these properties is demonstrated in their ability to describe the higher-order modes of optical fibers, more exotic vector beam, and the Pancharatnam-Berry GP for higher-order SOP.

We acknowledge financial support from Corning Inc. and the ARO. G.M. is greatly appreciative of helpful discussions with Joseph Birman.

---

\*ralfano@sci.ccny.cuny.edu

- [1] M. Born and E. Wolf, *Principles of Optics* (Cambridge University Press, Cambridge, England, 1999), 7th ed.
- [2] H. Poincaré, *Theorie Mathématique de la Lumière* (Gauthiers-Villars, Paris, 1892), Vol. 2.
- [3] R. H. Jordan and D. G. Hall, *Opt. Lett.* **19**, 427 (1994).
- [4] F. Gori, *J. Opt. Soc. Am. A* **18**, 1612 (2001).
- [5] Q. Zhan, *Adv. Opt. Photon.* **1**, 1 (2009).
- [6] A. Snyder and J. Love, *Optical Waveguide Theory* (Chapman and Hall, London, 1983).
- [7] L. Novotny *et al.*, *Phys. Rev. Lett.* **86**, 5251 (2001).
- [8] R. Dorn, S. Quabis, and G. Leuchs, *Phys. Rev. Lett.* **91**, 233901 (2003).
- [9] W. D. Kimura *et al.*, *Phys. Rev. Lett.* **74**, 546 (1995).
- [10] A. F. Abouraddy and K. C. Toussaint, *Phys. Rev. Lett.* **96**, 153901 (2006).
- [11] B. J. Roxworthy and K. C. Toussaint, *New J. Phys.* **12**, 073012 (2010).
- [12] A. Desyatnikov *et al.*, *Opt. Express* **18**, 10848 (2010).
- [13] C. Schwartz and A. Dogariu, *Opt. Lett.* **31**, 1121 (2006).
- [14] D. Huterer and T. Vachaspati, *Phys. Rev. D* **72**, 043004 (2005).
- [15] M. R. Dennis, K. O'Holleran, and M. J. Padgett, *Prog. Opt.* **53**, 293 (2009).
- [16] J. H. Poynting, *Proc. R. Soc. A* **82**, 560 (1909).
- [17] R. A. Beth, *Phys. Rev.* **50**, 115 (1936).
- [18] L. Allen *et al.*, *Phys. Rev. A* **45**, 8185 (1992).
- [19] C. Maurer *et al.*, *New J. Phys.* **9**, 78 (2007).
- [20] Q. Zhan, *Opt. Lett.* **31**, 867 (2006).
- [21] I. Freund, *Opt. Commun.* **201**, 251 (2002).
- [22] X.-L. Wang *et al.*, *Opt. Lett.* **32**, 3549 (2007).
- [23] J. D. Jackson, *Classical Electrodynamics* (Wiley, New York, 1999).
- [24] L. Allen, J. Courtial, and M. J. Padgett, *Phys. Rev. E* **60**, 7497 (1999).
- [25] A. M. Beckley *et al.*, *Opt. Express* **18**, 10777 (2010).
- [26] G. Milione *et al.*, *Proc. SPIE Int. Soc. Opt. Eng.* **7613**, 761305 (2010).
- [27] X.-L. Wang *et al.*, *Phys. Rev. Lett.* **105**, 253602 (2010).
- [28] S. Pancharatnam, *Proc. Indian Acad. Sci. A* **44**, 247 (1956).
- [29] G. Milione and R. R. Alfano, in *Frontier in Optics/Laser Science OSA*, Technical Digest (Optical Society of America, Washington, DC, 2010), paper FWC4.
- [30] R. Bhandari and J. Samuel, *Phys. Rev. Lett.* **60**, 1211 (1988).
- [31] R. Simon, H. J. Kimble, and E. C. G. Sudarshan, *Phys. Rev. Lett.* **61**, 19 (1988).
- [32] M. V. Berry, *Proc. R. Soc. A* **392**, 45 (1984).
- [33] M. V. Berry, *Curr. Sci.* **67**, 220 (1994).